Raman scattering in amorphous gallium antimonide

S. V. Demishev, Yu. V. Kosichkin, A. G. Lyapin, N. N. Mel'nik, D. V. Nekhaev, N. E. Sluchanko, and O. A. Turok

Institute of General Physics, Russian Academy of Sciences, 117942, Moscow
(Submitted 26 April 1993)
Zh. Eksp. Teor. Fiz. **104**, 2881–2893 (August 1993)

The Raman spectra of bulk samples of amorphous gallium antimonide prepared by quenching under pressure have been studied. Measurements were carried out over the frequency range 30 $cm^{-1} \leqslant \upsilon \leqslant 250$ cm^{-1}. The structure of the a-GaSb samples is highly disordered. The correlation length for optical vibrations is $L \sim 10$ Å. Measurements and an analysis of the shape of the spectral lines during the crystallization show that the spectrum retains a quasiamorphous structure even in a completely crystallized sample. A model is proposed for describing the changes in the shape of the Raman scattering line in the region of optical modes. In this model, a small correlation length arises because of the effect of the residual strain field. The relaxation of the residual stress field, which is manifested as an increase in the correlation length and the restoration of the Raman spectrum of a crystal, occurs during a recrystallization of a-GaSb samples. A photoinduced nonthermal formation of antimony inclusions has been observed. This process occurs above a threshold laser intensity. The nature of this effect may be governed by a radiation-stimulated aggregation of defects consisting of ruptured Ga–Ga and Sb–Sb bonds.

1. INTRODUCTION

Various noncrystalline materials prepared by solid-phase amorphization,[1] particularly bulk amorphous semiconductors prepared by quenching at high pressure,[1–3] have attracted increased interest over the past decade. Electrical, galvanomagnetic, and thermoelectric properties of such semiconductors have been studied.[2–5] The information available on their structure, however, is mostly limited to data from x-ray diffraction.[1–5] There have been only a few studies[6–8] in which the structure of amorphous GaSb produced by high pressure has been studied by the Raman scattering method. This method was used in Ref. 6, in experiments which revealed a disordering of the crystal structure of gallium antimonide as the result of a solid-phase amorphization. Raman scattering was used in Refs. 7 and 8 to study photocrystallization of a-GaSb. Lines of crystalline antimony were detected in these spectra. The latter result, however, was not confirmed by structural studies in Refs. 3 and 4.

Our purposes in the present study were to learn about the Raman spectra in bulk samples of gallium antimonide synthesized by quenching under pressure,[2–4] to investigate the thermally stimulated crystallization by the Raman method, and to learn about the effect of laser light on the structure of a-GaSb in the intensity in which there is no photostimulated crystallization.

The evolution of the Raman spectra in the course of the crystallization of an amorphous III-V semiconductor is a topic of independent interest. We know that in the case of the diamond-like semiconductor silicon the Raman spectra of the crystal c-Si and of the amorphous material a-Si are very different, because the correlation length of c-Si cannot be less than $L_c = 30$–40 Å, while that of a-Si is $L_a = 10$–15 Å (Ref. 9). As a result, a line of c-Si arises in the Raman spectra during the crystallization of a-Si along with a peak corresponding to optical vibrations in the amorphous network. The transformation of the spectra in the course of the crystallization can be summarized by saying that the amplitude of the "amorphous" line decreases, while that of the "crystal" line increases.

Semiconductors of the III-V group have the zinc blende structure, which differs from the diamond structure in that the two fcc sublattices are not identical as they are in the case of Si, but are instead formed by atoms of different groups. Since the structures of the crystalline phases of silicon and gallium antimonide are approximately the same, and since this is apparently true of their amorphous modifications, one is led to ask to what extent the changes in the Raman spectra characteristic of the crystallization of amorphous silicon are common to other tetrahedral amorphous semiconductors with a similar structure. To the best of our knowledge, this aspect of the problem has received essentially no study.

2. EXPERIMENTAL PROCEDURE

Samples of a-GaSb were synthesized in the setup described in detail in Ref. 3. The original single crystal of undoped GaSb (the GaSbI phase) was subjected simultaneously to a high pressure, $p_{syn} = 90$ kbar, and a high temperature, $T_{syn} \leqslant 1100$ °C. As a result, the sample was converted into a structure modification of the β-Sn type (GaSbII). The high-pressure phase GaSbII was then quenched at $p_{syn} = \text{const}$ to room temperature. The pressure was then reduced to atmospheric.

The inverse phase transition GaSbII → GaSbI led to the formation of the amorphous phase a-GaSb, with a short-range structure similar to that of GaSbI (Ref. 3). The disorder of the structure of the samples was monitored by

 1063-7761/93/080329-08$10.00

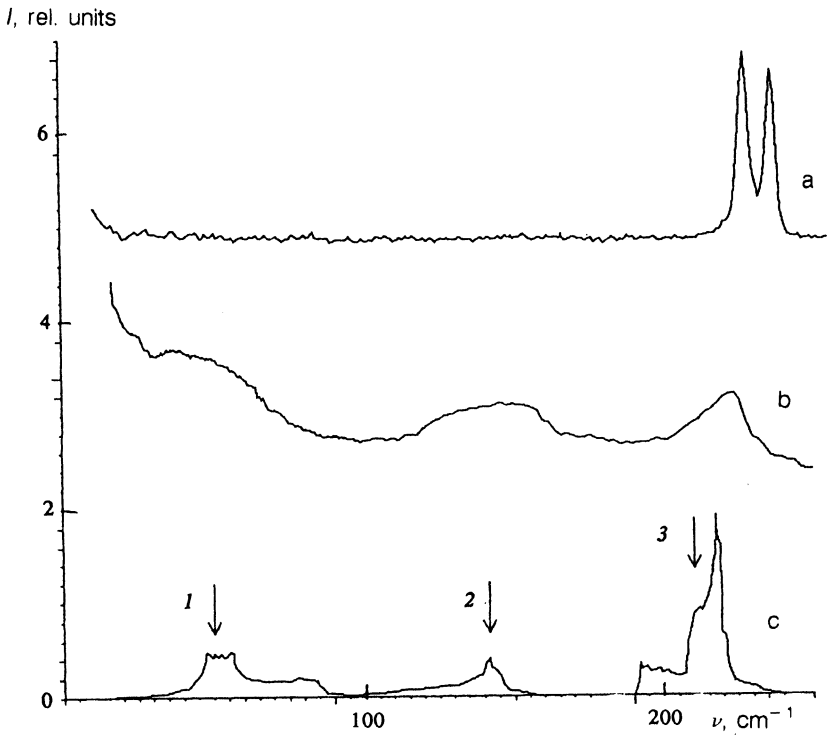

FIG. 1. Raman spectra of gallium antimonide. a—Single crystal; b—*a*-GaSb synthesized under pressure; c—model spectrum of vibrational states in gallium antimonide (in accordance with Ref. 10).

x-ray diffraction. Samples of *a*-GaSb in which the residual impurity of the crystalline phase GaSbI did not exceed 3–5% were selected for study.

The Raman spectra were recorded with a Jobin Yvon U-1000 spectrometer. The spectral resolution was 0.5–1 cm^{-1} at intensities of 10–40 W/cm^2. The Raman scattering was excited by an argon laser operating at a wavelength of 5145 Å. The diameter of the light spot on the sample was 200 μm. A microscope attachment made it possible to reduce the diameter of the illuminated region to 5–10 μm and to scan the light over the sample surface. The spectral characteristics of the apparatus were stabilized with the help of the silicon line at $v=521$ cm^{-1}. Silicon was the material of the substrate under the *a*-GaSb sample.

The *a*-GaSb samples were annealed in a multistep crystallization procedure. The sample was held at T_{ann} for 1 h in a helium atmosphere; then Raman spectra were recorded, as were curves of the intensity of the x-ray scattering (the Cu-K_α line was used). The structure factors $a(s)$, where $s=(4\pi/\lambda_0)\sin\theta$, λ_0 is the wavelength of the x radiation, and θ is the scattering angle, were determined from the cures of x-ray scattering intensity.[3,4] The temperature T_{ann} was then raised, and the measurement cycle repeated.

3. STRUCTURE OF THE RAMAN SPECTRA OF *a*-GaSb AND ITS CHANGES DURING THE CRYSTALLIZATION

Let us consider the overall structure of the Raman spectrum of GaSb. In crystalline samples, the TO mode corresponds to a frequency $v=228$ cm^{-1}, and the LO mode to $v=238$ cm^{-1} (Fig. 1a). For the amorphous samples of this semiconductor, *a*-GaSb, the spectral lines are highly broadened and contain three structural features (Fig. 1b): at 50, 150, and 224 cm^{-1}. Comparison with the curve of the density of states[10] of *c*-GaSb (Fig. 1c) reveals that these structural features correspond to peaks in the density of states for the following modes, respectively: TA (peak *1* in Fig. 1c), LA (peak *2* in Fig. 1c), and TO and LO (peak *3* in Fig. 1c).

The small correlation length in amorphous semiconductors causes a violation of the selection rules in terms of the phonon quasimomentum, and the Raman scattering spectrum $I(v)$ in the Stokes region reflects the entire density of vibrational states:[11]

$$I(v)=\sum_b C_b[1+n(v)]g_b(v)/v. \qquad (1)$$

The summation here is over all branches of the phonon spectrum; $n(v)$ is the Bose–Einstein factor; and C_b and g_b are respectively the coupling constant and the density of vibrational states for branch *b*. The appearance of structural features corresponding to acoustic modes in the Raman spectra thus confirms that the *a*-GaSb samples have undergone amorphization.

Interestingly, the Raman spectrum which we found for *a*-GaSb has no lines of crystalline antimony, in contrast with data in the literature.[7,8] A scan over the surface of a sample with the help of a microscope attachment showed that the shape of the $I(v)$ spectrum is independent of the particular point selected and that the samples are spatially uniform. In addition, the Raman spectrum of *a*-GaSb (Fig. 1b) is independent of the synthesis temperature T_{syn}, which was varied in the range 100–1100 °C. According to the results of Refs. 3 and 4, this independence means that we can rule out a contribution to the Raman spectra from regions with a local deviation from stoichiometry (accord-

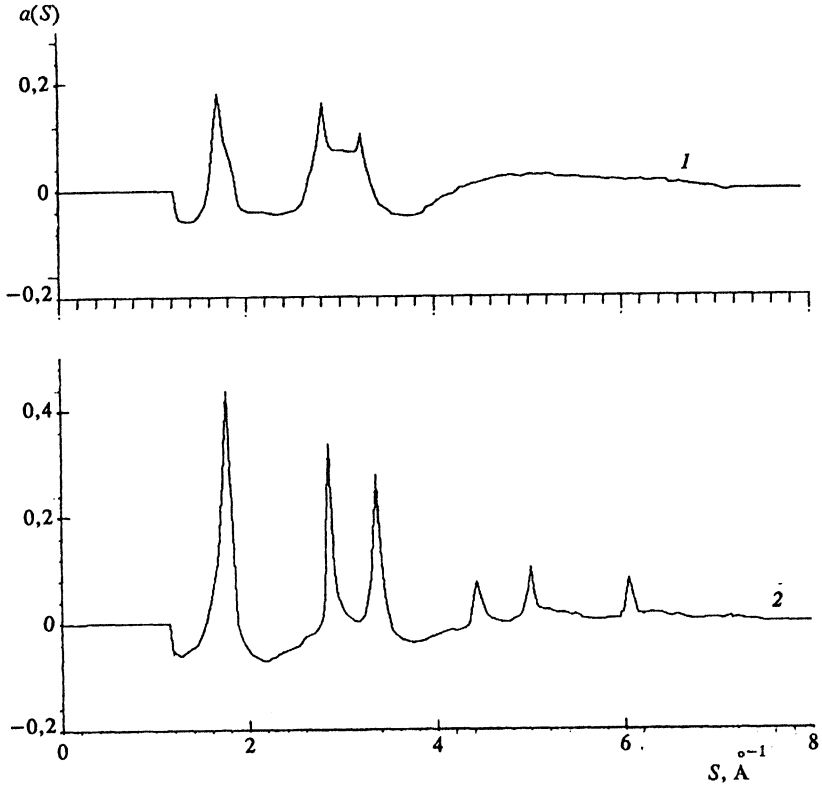

FIG. 2. X-ray-scattering structure factors of *a*-GaSb. *1*—Original sample; *2*—after annealing at $T_{ann}=420$ K.

ing to Refs. 3 and 4, deviations from stoichiometry occur at $T_{syn} > 800$ °C).

The Raman spectrum of *a*-GaSb is thus governed exclusively by the tetrahedral amorphous phase of gallium antimonide. The small residual crystal impurity (found by x-ray diffraction) also fails to make any significant contribution to this spectrum.

The results of the x-ray analysis (Fig. 2) and the differential thermal analysis (DTA) (Fig. 3) show that the crystallization of *a*-GaSb begins at $T_{ann} \approx 420$ K. This temperature corresponds to an intensification of the narrow $a(s)$ peaks corresponding to the crystalline phase *c*-GaSb, which we will refer to as "crystal" lines (Fig. 2), and to the beginning of a peak on the DTA curve (Fig. 3). The crystallization of the tetrahedral amorphous phase of *a*-GaSb terminates at $T_{ann} \approx 470$ K (Fig. 3; the main peak on the DTA curve).

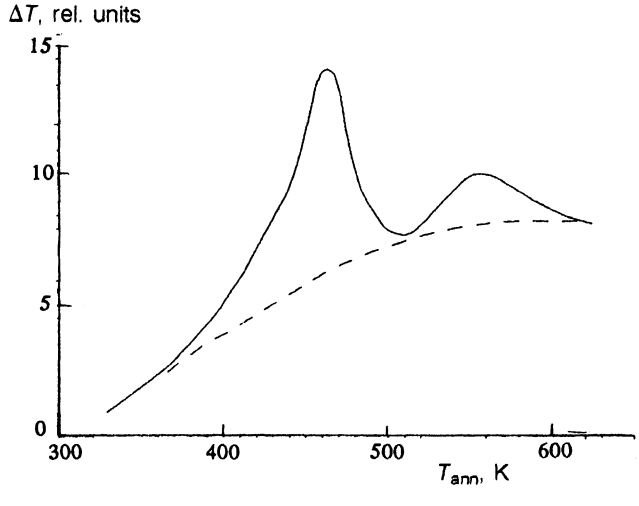

FIG. 3. Heat-evolution curve measured by differential thermal analysis for the amorphous semiconductor *a*-GaSb synthesized under high pressure. The dashed curve is a baseline.

A special study (reported in a separate communication) showed that the additional peak at $T_{ann} = 500$–600 K on the DTA curves is due to a recrystallization of polycrystalline GaSb formed as the result of the crystallization of *a*-GaSb.

The effect of annealing on the structure of the Raman spectra was investigated for the TO-like peak (Fig. 1a; curve *1* in Fig. 4), since only this structure feature is present in the spectra of both amorphous and crystalline GaSb.

No changes in the shape of the peak were found at temperatures up to $T_{ann} \approx 450$ K. The position of the TO peak is 224 cm^{-1}, and its half-width is 17 cm^{-1}. In the interval 450 K $\leqslant T_{ann} \leqslant$ 550 K we observe a progressive contraction and shift of the peak toward higher frequencies (curves *1* and *2* in Fig. 4). The position of the peak at $T_{ann} > 550$ K is 228 cm^{-1}. This position corresponds to a peak of the TO line in the spectrum of the crystal (Fig. 1; curve *3* in Fig. 4). A further increase in T_{ann} reduces the width of the peak to 6 cm^{-1}. At $T_{ann} \approx 590$ K, a TO–LO mode structure begins to appear (curve *4* in Fig. 4). The height of the LO peak is about 0.3 of that of the TO peak.

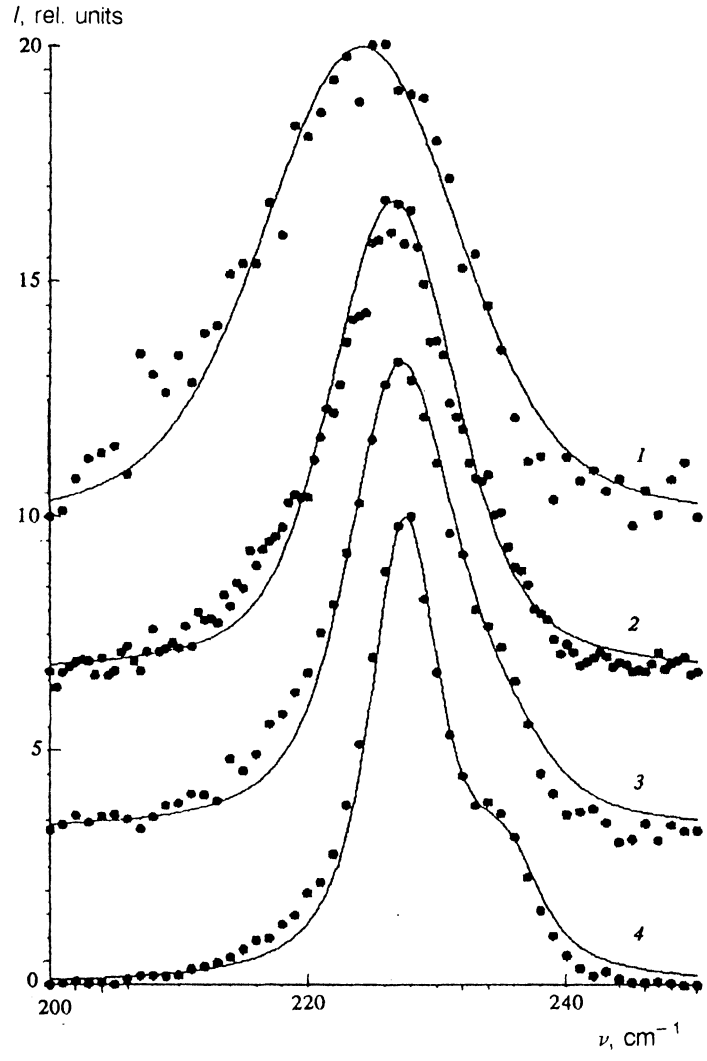

FIG. 4. Evolution of the *a*-GaSb Raman spectrum in the region of optical modes in the course of annealing. Points—Experimental; lines—calculated from a model (see the text proper). *1*) $T_{ann}=470$ K; *2*) 530 K; *3*) 550 K; *4*) 590 K.

At annealing temperatures of 550–620 K, the LO feature is observed at $v=232$–234 cm^{-1} (Fig. 4).

The evolution of the Raman spectrum of *a*-GaSb in the course of the crystallization is thus radically different from the process characteristic of *a*-Si. In the case of *a*-GaSb synthesized at high pressure there is a progressive change in the shape of the spectral line. Furthermore, at those T_{ann}'s at which the *a*-GaSb sample has already crystallized completely (Figs. 2 and 3), the TO–Lo mode structure is not resolved. The spectrum retains its "amorphous" shape (Fig. 4).

This result shows that it is generally not possible to assert that an experimental entity has undergone amorphization on the sole basis of the shape of the Raman spectra in a limited spectra interval. Determining the extent of amorphous structure requires the use of other methods for studying structure.

We wish to stress that for *a*-GaSb the correlation length of the amorphous network calculated from the $a(s)$ curves (Fig. 2) is $L_a\approx 20$ Å, while at a temperature as low as $T_{ann}\approx 420$ K the size of the crystallites is $L_c\approx 200$ Å (this estimate was based on an analysis of the shape of the crystalline lines). Further crystallization increases the size of the crystallites, but even after the crystallization has gone to completion the relation $L_c \gg L$ continues to hold, where L is the correlation length for vibrational states. This is an extremely unusual behavior, since L and L_c are usually assumed to be comparable in order of magnitude.[12,13] Only at $T_{ann}\approx 600$ K does the correlation length increase to the extent that a TO–LO splitting is observed in the Raman spectra (Fig. 4).

For a quantitative analysis of the shape of the Raman line (Fig. 4) we used the following model. The phonon wave function in a disordered system can be written[12]

$$\psi(\mathbf{k}_0,\mathbf{r})=A\exp(-2r^2/L^2)\Phi(\mathbf{k}_0,\mathbf{r}), \tag{2}$$

where $\Phi(\mathbf{k}_0,r)=u(\mathbf{k}_0,\mathbf{r})\exp(-i\mathbf{k}_0\mathbf{r})$ is the phonon wave function in an infinite crystal, and $\mathbf{k}_0$ is the quasimomentum. If we ignore the difference between the lifetimes and the polarizability constants for different values of the quasimomentum, we find that the shape of a spectral line is given by

$$I^*(v)\propto\int\frac{|c(0,\mathbf{k}|^2 d^3\mathbf{k}}{[v-v_0(\mathbf{k})]^2+\Gamma_0^2/4}, \tag{3}$$

where $c(\mathbf{k}_0,\mathbf{k})$ is

$$c(\mathbf{k}_0,\mathbf{k})=\frac{AL}{(2\pi)^{3/2}}\exp\left[-\frac{L^2}{8}(\mathbf{k}-\mathbf{k}_0)^2\right]. \quad (4)$$

This quantity is a coefficient of a plane-wave expansion of wave function (2). In (2), $v_0(\mathbf{k})$ is the phonon dispersion law, and the parameter Γ_0 is determined by the phonon lifetime.

As in the case of silicon,[14] we use a harmonic approximation for $v_0(k)$:

$$v_0(k)=K_1+K_2\cos\left(\frac{\pi k}{k_b}\right). \quad (5)$$

Here k_b is the wave vector of the Brillouin zone. The sum K_1+K_2 gives use the value of the frequency for $k=0$, while the difference K_1-K_2 determines the frequency at the boundary of the Brillouin zone.

Using data in the literature[10] on GaSb, we find the following results for the TO and LO modes:

$$K_1^{TO}+K_2^{TO}=228\ \text{cm}^{-1},\quad K_1^{TO}-K_2^{TO}=210\ \text{cm}^{-1},$$

$$K_1^{LO}+K_2^{LO}=238\ \text{cm}^{-1},\quad K_1^{LO}-K_2^{LO}=206\ \text{cm}^{-1}.$$

We thus find $K_1^{TO}=219\ \text{cm}^{-1}$, $K_2^{TO}=9\ \text{cm}^{-1}$, $K_1^{LO}=222\ \text{cm}^{-1}$, and $K_1^{LO}=14\ \text{cm}^{-1}$.

In the standard models[12,13] the quantity L_c is determined by the vibration conditions at a boundary between blocks, which are different for the LO and TO modes. In the case $L_c\gg L$, the boundary-condition question is not as evident. Nevertheless, in approximating the experimental data we will consider the general case in which the correlation lengths L_{TO} and L_{LO} are different.

It follows from (2)–(4) that the quantity Γ_0 is determined by the lifetime of the LO and TO phonons. The value of Γ_0 was thus found from the lineshape of the original crystalline sample (curve *1* in Fig. 1). When the parameter Γ_0 is determined in this way, it obviously includes the instrumental broadening. The best agreement with experiment was reached for a Lorentzian line, (4), with $\Gamma_0^{TO}\approx 5\ \text{cm}^{-1}$ and $\Gamma_0^{LO}\approx 4\ \text{cm}^{-1}$.

A second mechanism shaping the Raman peak stems from the anharmonic shift Δv of the Raman spectral line of a crystallite upon deformation. Denoting by X the stress during hydrostatic compression, we have[15]

$$\Delta v=\frac{X(p+2q)(S_{11}+2S_{12})}{2v_0}=3X(S_{11}+S_{12})\gamma v_0, \quad (6)$$

where v_0 is the position of the peak in the case $X=0$, p and q are anharmonic constants, $\gamma=(p+2q)/6v^2$, and S_{11} and S_{12} are elastic constants. The values $\gamma=1.10\pm 0.22$ and $S_{11}+2S_{12}=0.59\cdot 10^{-12}\ \text{cm}^2/\text{dyn}$ were found for GaSb in Ref. 15. From (6) we then find the estimate

$$\Delta v=BX\ \text{cm}^{-1}, \quad (7)$$

where X is in units of dyn/cm^2, and $B=4.6\cdot 10^{-10}$.

We make the further assumption that the average force acting on a crystallite is zero. In other words, the numbers of compressed and stretched crystallites are the same. Evidence for this conclusion comes from the fact that the density of the *a*-GaSb samples is close to that of a crystal.[4] We further assume that the stress distribution and thus the distribution of the shifts Δv among crystallites are Gaussian. In our model the half-width of the Gaussian distribution of the shifts $\Delta\Gamma$ must be the same for the TO and LO modes, since the corresponding anharmonic constants are equal.[15]

The resultant Raman lineshape in our model is found by convolving function (3) with a Gaussian function with a half-width at half-maximum $\Delta\Gamma/2$. The latter function serves as a model of inhomogeneous broadening due to deformation:

$$I(v)=\sum_b A_b\int I^*(v-v')\exp\left[-\frac{v'^2\ln 2}{(\Delta\Gamma/2)^2}\right]\frac{dv'}{\Delta\Gamma}. \quad (8)$$

The summation here is over all branches of optical vibrations. The ratio A_{LO}/A_{TO} was found at the maximum annealing temperature, where it was $A_{LO}/A_{TO}\approx 0.22$.

We are thus left with three adjustable parameters in our model: L_{TO}, L_{LO}, and $\Delta\Gamma$. The solid lines in Fig. 4 are fits of expression (8) to the experimental data. We see that the model proposed here gives a good description of the shape of the Raman line of GaSb in the region of optical modes.

Figure 5 shows L_{TO}, L_{LO}, and $\Delta\Gamma$ versus the annealing temperature. At $T_{ann}<450$ K the half-width $\Delta\Gamma=13\ \text{cm}^{-1}$ and $L_{TO}=10$ Å are essentially independent of T_{ann}. Using (7), we find the characteristic compressional stress to be $X\approx 3\cdot 10^{10}\ \text{dyn/cm}^2$. This figure corresponds to a change $\Delta a/a=0.02$ in the interatomic distance. In the interval 450 K $<T_{ann}<$ 550 K we observe a decrease in $\Delta\Gamma$ and an increase in L_{TO}. At higher temperatures, 550 K $<T_{ann}<$ 620 K, some TO–LO structure appears, $\Delta\Gamma$ decreases to 3 cm^{-1}, L_{TO} increases to 50–60 Å, and the parameter L_{LO} increases from 8 Å to 12 Å. We wish to stress that when the correlation lengths are equal, $L_{LO}=L_{TO}$, it is not possible to find a satisfactory approximation of the shape of the Raman line of GaSb.

Interestingly, the beginning of the increase in the correlation length L_{TO} coincides with the beginning of the recrystallization process, while the decrease in $\Delta\Gamma$ occurs over the entire T_{ann} range, beginning at $T_{ann}\approx 450$ K (Fig. 5). The crystallization of the amorphous phase in *a*-GaSb thus leads to a decrease in the local stress, while the correlation length which specifies the asymptotic behavior of the phonon wave function remains constant up to $T\approx 500$ K. At $T_{ann}>500$ K, where recrystallization occurs, the correlation length increases, and the stresses simultaneously decrease. The data found by modeling the lineshape in the Raman spectrum thus confirm the qualitative conclusion, formulated above, that the correlation lengths L_{TO} and L_{LO} and the size of a crystallite differ substantially.

In this situation, under the inequalities L_{TO}, $L_{LO}\ll L_c$, the standard interpretation of correlations lengths on the basis of the microcrystal model[13] runs into serious trouble. However, an approach according to which L_{TO} and L_{LO} are limited by the size of a crystallite is not the only approach possible. One might suggest that the parameters

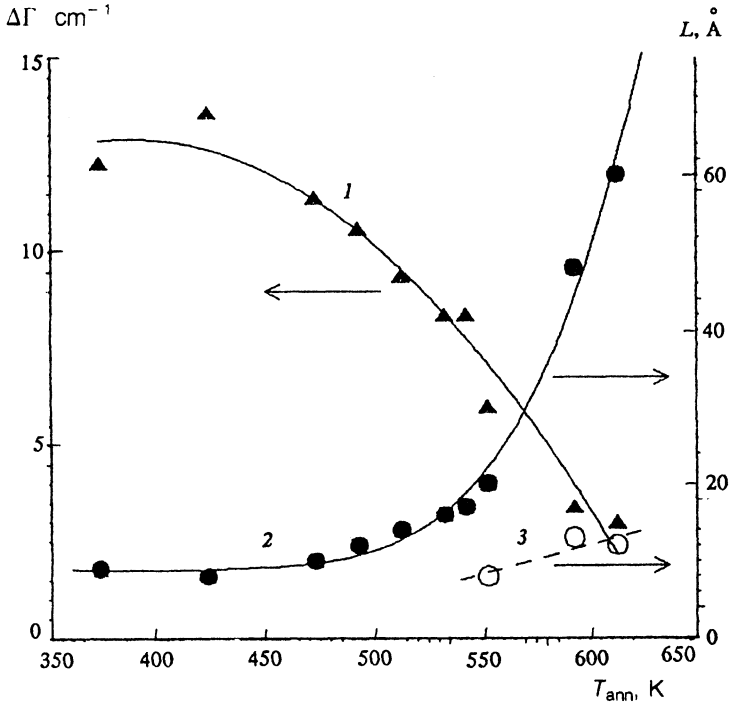

FIG. 5. Parameters of the model as a function of the annealing temperature. *1*—$\Delta\Gamma$; *2*—L_{TO}; *3*—L_{LO}.

L_{TO} and L_{LO}, which determine the coherence length for the wave function for the TO and LO phonons, are set by the same random local stress field which determines the value of $\Delta\Gamma$. In this case the data in Fig. 5 would mean that there is initially a decrease in the absolute value of the stress in *a*-GaSb without a change in structure, as is reflected in a constant value of L_{TO} and a decrease in $\Delta\Gamma$. With increasing T_{ann}, the stress in the sample relaxes, and L_{TO} begins to increase (Fig. 5).

Along that approach we do not find an explanation of the difference between the correlation lengths for the TO and LO modes, while this difference can be explained in a natural way in the microcrystal model with boundary conditions at the surface of a crystallite.[12,13] The construction of a model capable of describing the experimental data on *a*-GaSb (Figs. 4 and 5) will apparently require further theoretical work.

4. PHOTOSTRUCTURAL CONVERSIONS IN *a*-GaSb

The following experimental procedure was used to learn about the effect of the intensity of the laser light on the Raman spectrum of the amorphous semiconductor *a*-GaSb synthesized under high pressure. For a time interval $\Delta t=1$ min the sample was exposed to a laser beam of intensity P. The intensity was then lowered to a value at which no changes occurred in the spectrum, and the Raman spectrum was recorded. The intensity P was then raised, and the measurement cycle repeated.

The results of one such experiment are shown in Fig. 6. At $P<P_c\approx 13$ W/cm^2 the structure of the Raman spectrum is independent of the light intensity, and $I(v)$ has the shape described in the preceding section of this paper (curve *1* in Fig. 6a). When P exceeds a critical value, $P>P_c$, intense lines similar to those observed in Refs. 7 and 8 appear at $v\approx 150$ cm^{-1}. These lines are due to TO and LO modes for crystalline antimony.

To obtain a quantitative characteristic of the effect we used the line amplitude ratios $A(v=150\ \text{cm}^{-1})/A_0$ (antimony) and $B(v=224\ \text{cm}^{-1})/B_0$ (the TO peak of *a*-GaSb). Here A_0 and B_0 are the intensities corresponding to the LA and TO modes in the original *a*-GaSb spectrum. Figure 6b shows plots of $A(P)$ and $B(P)$. We clearly see a threshold for the effect. The photoinduced formation of antimony inclusions is observed in an intensity interval in which there is essentially no crystallization of the *a*-GaSb phase [a photoinduced crystallization of *a*-GaSb is manifested as an increase in the amplitude $B(P)$].

The observed effect is specific to the amorphous phase of GaSb, since in the case of the crystal an increase in the intensity to the highest level possible in our experiments, $P\sim 200$ W/cm^2, did not result in the appearance of antimony lines. Moreover, it follows from data on the thermal crystallization of GaSb that annealing at the highest values T_{ann} does not lead to the appearance of antimony lines, and it does not disrupt the phase composition of the samples. The process by which antimony inclusions segregate during the application of laser light is thus not a thermal process.

Annealing an *a*-GaSb sample with antimony inclusions formed after illumination revealed that this structural transformation of the samples is irreversible. Furthermore, annealing at $T_{ann}=400$ K for 90 min raised the intensity of the peak at $v=150$ cm^{-1} by a factor of more than 2.

The data obtained on the photoinduced formation of antimony inclusions in *a*-GaSb can be interpreted at a qualitative level in the following model. In the case of an amorphous material of the III-V group there is an ex-

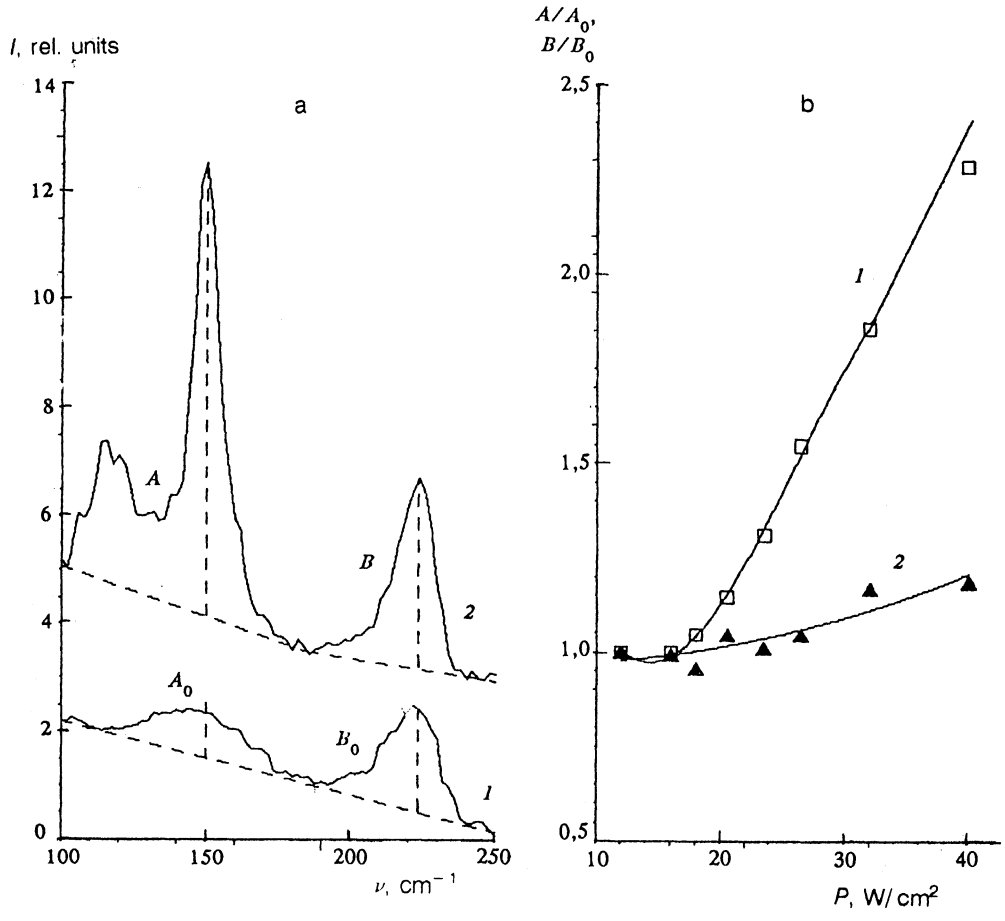

FIG. 6. Effect of the laser light intensity on the Raman spectrum of a-GaSb. a: Structure of spectrum. *1*—Original sample; *2*—after illumination at a power density $P=32$ W/cm^2. b: *1*—$A(P)/A_0$; *2*—$B(P)/B_0$.

tremely high probability for finding structural defects of the A–A and B–B types (in the case of a-GaSb, Ga–Ga, and Sb–Sb bonds). Such defects are specific to the amorphous phase of these materials[16] and are not characteristic of the crystal. Intense laser light can excite a radiation-stimulated diffusion[17] of such defects. The activation energy for a radiation-stimulated diffusion is typically low (or even zero),[17] so this process proceeds much faster than the thermally activated diffusion. This difference in rates explains the nonthermal nature of the effect.

As a result, the mobility of defects of the Ga–Ga and Sb–Sb type increases sharply. A spatial aggregation of such defects apparently results in the formation of Ga and Sb inclusions on the surface of an a-GaSb sample. Only the antimony inclusions contribute significant lines, since gallium is a typical metal, and the Raman scattering by a gallium inclusion would be of low intensity.

This model also makes it a simple matter to explain the increase in the height of the peak at $\upsilon=150$ cm^{-1} upon annealing. It is natural to expect that both ordered and disordered a-Sb phases can form during aggregation of Sb–Sb defects. The crystallization temperature of a-Sb is given in the literature;[18] it is low, $T_{cr}=240$–313 K. Accordingly, the appearance of intense crystalline lines of antimony may be due to a photocrystallization of a-Sb inclusions formed during diffusion. A thermal crystallization of a-Sb inclusions would also induce an increase in the height of these lines, and such an increase is observed experimentally.

It may be that the threshold P_c, which characterizes the anomalous diffusion (Fig. 6b), is low in comparison with that of a crystal not only because of specific defects but also because of the presence of stressed regions (Sec. 3). A stress relaxation due to the application of light might constitute an additional source of the energy required for the appearance of diffusion anomalies and the resulting photoinduced formation of antimony inclusions.

5. CONCLUSION

In summary, it has been shown here that a solid-phase amorphization of GaSb samples at high pressure results in a pronounced disordering of their structure. In the case of vibrational states, the disordering is manifested by a decrease in the correlation lengths to values $L\sim 10$ Å. As a result, the selection rule on the quasimomentum is lifted, so there is a substantial line broadening in the Raman spectra in the region of the optical TO and LO modes, $\upsilon=210$–240 cm^{-1}. In addition, a structural peculiarity associated with an LA mode ($\upsilon=150$ cm^{-1}) appears in the spectrum.

The result that the correlation lengths $L=10$–20 Å do not change even after the crystallization of the tetrahedral amorphous phase has gone to completion was unexpected,

as was the result that the Raman spectrum of a polycrystalline GaSb sample retains a shape typical of that of the original *a*-GaSb sample. This behavior might be explained on the basis that the correlation length is small in this case because of the effect of a random strain field. A stress relaxation and thus an increase in the correlation length occur in the region in which the test samples recrystallize.

A study of the effect of laser light on the structure of the amorphous semiconductor *a*-GaSb synthesized at high pressure revealed a photoinduced nonthermal formation of antimony inclusions when the light intensity exceeded a certain critical value. This effect arises at light intensities at which there is no photocrystallization of *a*-GaSb. It may be due to an aggregation of Sb–Sb defects as the result of an anomalous radiation-stimulated diffusion.

[1] E. G. Ponyatovsky and O. I. Barkalov, Mater. Sci. Rep. **8**, 147 (1992).
[2] S. V. Demishev, Yu. V. Kosichkin, A. G. Lyapin *et al.*, J. Non-Cryst. Solids **97/98**, 1459 (1987).
[3] S. V. Demishev, Yu. V. Kosichkin, D. G. Lunts *et al.*, Zh. Eksp. Teor. Fiz. **100**, 707 (1991) [Sov. Phys. JETP **73**, 394 (1991)].
[4] V. V. Brazhkin, S. V. Demishev, Yu. V. Kosichkin *et al.*, Zh. Eksp. Teor. Fiz. **101**, 1908 (1992) [Sov. Phys. JETP **74**, 1020 (1992)].
[5] V. F. Degtyareva, I. T. Belash, E. G. Ponyatovskiĭ, and V. I. Rasshupkin, Fiz. Tverd. Tela (Leningrad) **32**, 1429 (1990) [Sov. Phys. Solid State **32**, 834 (1990)].
[6] V. I. Larchev, N. N. Kel'nik, S. V. Popova *et al.*, Kratk. Soobshch. Fiz., No. 1, 7 (1985).
[7] V. N. Denisov, B. N. Mavrin, V. B. Podobedov, and G. G. Skrotskaya, Pis'ma Zh. Eksp. Teor. Fiz. **50**, 363 (1989) [JETP Lett. **50**, 393 (1989)].
[8] S. V. Popova, G. G. Skrotskaya, V. I. Larchev *et al.*, J. Non-Cryst. Solids **135**, 255 (1991).
[9] M. Cardona (editor), *Light Scattering in Solids*, Springer-Verlag, New York, 1975.
[10] V. K. Farr, J. G. Traylor, and S. K. Sinha, Phys. Rev. B **11**, 1587 (1975).
[11] R. Shuker and R. Gamon, Phys. Rev. Lett. **25**, 222 (1970).
[12] H. Richter, Z. P. Wang, and L. Ley, Solid State Commun. **39**, 625 (1981).
[13] I. H. Campbell and P. M. Fauchet, Solid State Commun. **58**, 739 (1986).
[14] J. L. Birman, *Theory of Crystal Space Groups and Lattice Dynamics*, Springer-Verlag, New York.
[15] F. Cerdeira, C. J. Buchenauer, F. H. Pollak, and M. Cardona, Phys. Rev. B **5**, 580 (1972).
[16] D. Udron, M.-L. Theye, D. Raoux *et al.*, J. Non.-Cryst. Solids **137/138**, 131 (1991).
[17] T. D. Dzhafarov, *Radiation-Stimulated Diffusion in Semiconductors*, Energoatomizdat, Moscow, 1991, p. 183.
[18] V. A. Shklovskiĭ and V. M. Kuz'menko, Usp. Fiz. Nauk **157**, 311 (1989) [Sov. Phys. Usp. **32**, 163 (1989)].

Translated by D. Parsons